DAEHAN HWAHAK HWOEJEE
(*Journal of the Korean Chemical Society*)
Vol. 23, No. 1, 1979
Printed in Republic of Korea

결합공간과 반결합공간 (제 2 보). H_2O_2의 C_2H_6의 Internal Rotation Barrier의 원천적 요인

金鎬濟 · 李德煥
서울대학교 자연과학대학 화학과
(1978. 11. 22 접수)

Bonding and Antibonding Regions (II). Origin of Barriers to Internal Rotation of H_2O_2 and C_2H_6

Hojing Kim and **Duckhwan Lee**
Department of Chemistry, Seoul National University, Seoul 151, *Korea*
(Received Nov. 22, 1978)

요 약. 과산화수소와 에탄의 internal rotation barrier의 원천적 요인을 결합 공간과 반결합 공간의 개념을 이용하여 연구하였다. internal rotation barrier는, 중심 원자의 존재로 인하여 전이밀도가 중심 원자가 없을 때보다 더 많이 반결합 공간으로 쏠림에 기인 함을 밝혔다. 이러한 전이밀도의 쏠림은 강한 O-H (또는 C-H) 결합에 의하여 내부 회전에 따른 전자밀도의 변화가 적어지는 것으로 설명할 수 있음을 보였다.

ABSTRACT. The origin of barriers to internal rotation of hydrogen peroxide and ethane is investigated by using the concept of Bonding and Antibonding Regions. The strong bond formations between the axial and end atoms on the same side make the real charge densities in these molecules less dependent on conformations than those in the hypothetical molecules having no axial atoms. Thus, the existence of the axial atoms should induce the migration of the transition density from the Bonding region to the Antibonding region. Barrier to internal rotation can be understood in terms of this migration of the transition density to such an extent that the change in nuclear-nuclear repulsion energy becomes the dominating part of the total perturbation energy.

1. INTRODUCTION

Barrier to internal rotation has been one of the most interesting subjects to chemists, ever since it was found in 1936.[1] It is very important to understand the nature of the barrier, which is related to the conformational and biological activity of large molecule. The barrier heights have been successfully evaluated for small molecules by SCF scheme[2~5] or perturbation theory.[6]

Early in 1960's, Clinton,[7a] Karplus and Parr,[7b] and Ruedenberg[7c] showed that the difference of the nuclear repulsion energy yields a barrier of the correct sign and magnitude. Thereafter, in the effort to search the barrier ori-

gin, the total perturbation energy accompanying the conformational change has been partitioned into various components and the major contributing component to barrier has been sought.[5,8,10] Wyatt and Parr[8] suggested, through the use of the Integral Hellmann-Feynman Theorem (IHF),[9] that the change of the electronic energy of ethane comes mainly from the three-fold transition density component in the vicinity of protons. Fink and Allen[5] attempted to analyze the barrier mechanism by the partition of the total energy into one- and two-electron components. Allen[10] classified the barriers as the attractive and repulsive dominant, and discussed the nature of the barriers of ethane and acetaldehyde by using the electron-density-distribution plots.[11]

Another approach to the barrier origin is based on the localized bond orbital descriptions.[12,13] In 1968, Sovers *et al.*[12a] pointed out from the simple bond-function analysis that the orbital orthogonality, which is introduced by the Pauli Exclusion Principle, is the prime factor in the rotational barrier of ethane. They extended the similar analysis to methanol in 1974.[12b] These results have been reconfirmed by many other workers.[13]

In this paper, we attempt to give a new and simple interpretation of the barrier orign by partitioning the total perturbation energy (ΔE) into the change of the nuclear-nuclear repulsion energy (ΔE_{nn}) and that of the electronic energy (ΔE_{el}) using IHF. It may be easily shown from the experimental results of barriers that ΔE_{nn}, in general, has an opposite phase to ΔE_{el}, which is less than ΔE_{nn} in absolute value. Namely, ΔE_{el} attenuates ΔE_{nn} as pointed out by Karplus *et al.*[7] Thus the origin of the internal rotation barrier might be comprehended not by seeking the major component of ΔE_{el} (or ΔE), but by answering the most fundamental question: "Why is the magnitude of ΔE_{el} less than that of ΔE_{nn}?" To do so, we introduce the new concept of the Bonding and Antibonding Regions,[14] and compare the transition density[15] of the actual molecule with that of the hypothetical molecule which has the same nuclear framework except the axial atoms and has the same perturbation opertors, $\Delta v(1)$ and ΔV_{nn}.[16]

The concept of the Bonding and Antibonding Regions is briefly outlined in Section 2. In Sec. 3, the barrier origin of H_2O_2, which has a reatively large barrier and has a realistic reference molecule, H_2, is analyzed by using this concept. The barrier of ethane is discussed from the same viewpoint.

2. BONDING AND ANTIBONDING REGIONS

Only a short outline of the Bonding and Antibonding Regions will be given here since full details can be found in Paper I.[14] We will use the same notations as in Paper I without any further comments.

According to IHF, the perturbation energy due to the change of the nuclear framework from R_0 to R is given by

$$\Delta E(R_0 \rightarrow R) = \int \Delta v(1)\, \rho_{R_0 R}(1)\, d\tau_1 + \Delta E_{nn}(R_0 \rightarrow R) \equiv \Delta E_{el}(R_0 \rightarrow R) + \Delta E_{nn}(R_0 \rightarrow R) \quad (1)$$

Transition density, $\rho_{R_0R}(1)$, is positive definite and can be approximated to the average real charge density, $\frac{1}{2}(\rho_{R_0R_0}(1)+\rho_{RR}(1))$. This approximation seems to be a good one in all space except the vicinity of nuclear sites. Thus, one can guess the general pictures of the real charge densities from the fictitious transition density.

From the positive-definiteness of the transition density, one can divide the transition density space into the Bonding and Antibonding

Regions solely by the sign of $\Delta v(1)$:

$$\Delta E_{el}(R_0 \rightarrow R) = \int_{\Delta v(1)<0} \Delta v(1)\rho_{R_0R}(1)d\tau_1 \quad \text{(negative)} + \int_{\Delta v(1)>0} \Delta v(1)\rho_{R_0R}(1)d\tau_1 \quad \text{(positive)} \qquad (2)$$

The boundary surfaces of these two regions are given by the solutions of $\Delta v(1)=0$. The transition charge element $\rho_{R_0R}(1)d\tau_1$ in the Bonding Region contributes to the lowering of energy, and $\rho_{R_0R}(1)d\tau_1$ in the Antibonding Region acts in the opposite way during the change of the nuclear framework from R_0 to R.

3. RESULTS AND DISCUSSIONS

The hydrogen peroxide molecue, H_2O_2, which may be the simplest molecule having the barrier to internal rotation, has moderately high symmetry so that one is able to prove the existence of the extreme values of E_{el}, E_{nn}, and E at both *trans* and *cis* conformations without an explicit use of the wavefunctions. However, it has fairly larger barrier[18] in comparison with such prototype molecules listed in *Table* 1. Thus, under small modifications in bond lengths and wavefunctions caused by scaling,[5] the relative phase and amplitude of $E_{el}(=E_T+E_{ee}+E_{ne})$ and E_{nn} are considered to be invariant. The facts thus validate the partition of the total energy E into E_{el} and E_{nn}. And the partition is compatible with the use of IHF formula of Eq. (1) to be used in the following discussions. Lastly, and the most important of all, the moving part of the molecule in the process of the internal rotation has a realistic analogue, H_2 molecule, as long as the perturbation operators, $\Delta v(1)$ and ΔV_{nn}, are concerned.

Table 1. Barrier to internal rotation[a].

	E_{exp}[b]	E_{nn}[c]	E_{el}[d]
CH_3CH_3	2.88	4.70	−1.82
CH_3CF_3	3.25	52.17	−48.92
CH_3CCl_3	2.91	112.55	−109.64
CH_3SiH_3	1.70	3.32	−1.62
CH_3SiF_3	1.40	30.23	−28.83
CH_3NH_2	1.98[e]	2.55[e]	−0.57
CH_3OH	1.06	1.10[f]	−0.04
CH_3SH	1.27	1.86	−0.59
H_2O_2(*cis*)	7.0[g]	56.2[h]	−49.2
H_2S_2(*cis*)	6.9[i]	39.6[i]	−32.7

[a]in kcal/mole, [b]experimental values are taken from Ref. 13 unless otherwise stated, [c]calculated from the data in Ref. 19 unless otherwise stated, [d]$\Delta E_{el}=\Delta E_{exp}-\Delta E_{nn}$, [e]see Ref. 5b, [f]see Ref. 5a, [g]see Ref. 18, [h]see Ref. 20, [i] see Ref. 3c.

For the purpose of analysis, *trans* and *cis* H_2O_2 are arranged to a space-fixed coordinate system[4] as in *Fig.* 1. At the same time, H_2 molecules, which have exactly equivalent protonic configurations to the *trans* and *cis* H_2O_2 (and will be called hereafter as *trans* and *cis* H_2, respectively) are similarly arranged to the coordinate systems. Assuming a hypothetical situation in which the protons originally at the

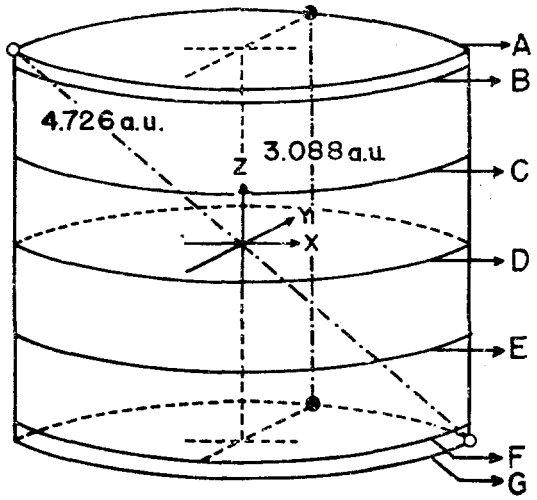

Fig. 1. Coordinate systems of *cis* (●) and *trans* (○) H_2O_2. Sections A and G include protons. Sections C and E are the center of the molecule at the origin. Section D is xy-plane. The internuclear separation of two oxygens is 2.787 a.u.

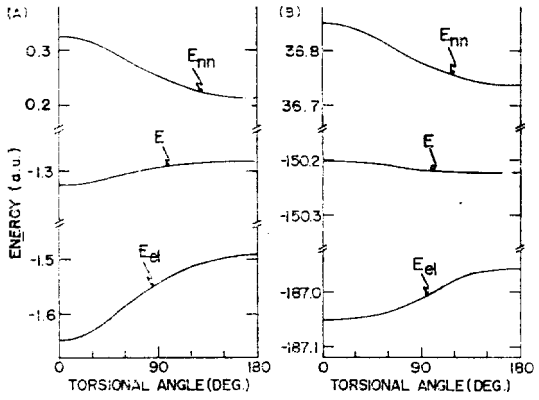

Fig. 2. (A) Energy *vs.* torsoinal angle of H_2 obtained from the calculations of McLean *et al.* by constraining protons on Sections A and G. (B) Schematic energy diagram *vs.* torsional angle of H_2O_2 obtained from SCF calculations by Pitzer and Palke.

trans positions (R_0=4.726 a.u.) move along the circular paths in Sections A and G up to the *cis* positions (R=3.088 a.u.), one can depict the energy *vs.* torsional angle, ω, instead of the internuclear separation, as given in *Fig.* 2 (A). *Fig.* 2(B) shows the energy dependence of H_2O_2 on the torsional angle and is plotted using Pitzer's values.[4] Although the Pitzer's calculation has failed to show the existence of the *trans* barrier, and has given a relatively poor numerical value of barrier (13.05 kcal /mole), it does show the correct phase of E_{el} and E_{nn}. Since the primary purpose of the present analysis is to see "why is $\Delta E(trans\rightarrow cis)>0$ in H_2O_2?" rather than the actual value of the barrier height itself, the use of the Pitzer's values does not impose any limit on the following discussions. Comparison of *Figs.* 2(A) and (B) reveals that the axial atoms, oxygens, are responsible for the dampening effect on the decrease of E_{el} during the conformational change from *trans* to *cis* and thus the barrier is created in the *cis* positions, or $\Delta E(trans\rightarrow cis)>0$.

The situation may be better understood

Table 2. Energy changes in internal rotation.[a]

	E_{calc}[b]	E_{nn}	E_{el}[c]
H_2O_2[d]	13.05	70.44	−57.39
H_2[e]	−26.66	70.44	−97.10
C_2H_6[f]	3.28	4.70	−1.42
H_6[g]	−16.78	4.70	−21.48

[a]in kcal/mole, [b]calculated barrier height, [c]$\Delta E_{el}=\Delta E_{calc}-\Delta E_{nn}$, [d]see Ref. 4, [e]energy changes during the same protonic framework change of H_2O_2 are calculated from the data in Ref. 17, [f]see Ref. 2, [g]energy changes during the same nuclear framework change of C_2H_6 are obtained from our CNDO calculations.

throngh *Table* 2 and the energy formulae:

$$\Delta E^{H_2}(trans\rightarrow cis)=\int \Delta v(1)\rho_{tc}^{H_2}(1)\,d\tau_1 + \Delta E_{nn}(trans\rightarrow cis) \quad (3)$$

$$\Delta E^{H_2O_2}(trans\rightarrow cis)=\int \Delta v(1)\rho_{tc}^{H_2O_2}(1)\,d\tau_1 + \Delta E_{nn}(trans\rightarrow cis) \quad (4)$$

where ΔE_{nn} and $\Delta v(1)$ are common to H_2 and H_2O_2, and

$$\Delta v(1)=\left\{-\sum_{k=1}^{2}\frac{1}{r_{k_1}}\right\}-\left\{-\sum_{m=1}^{2}\frac{1}{r_{m_1}}\right\} \quad (5)$$

(*cis* protons) (*trans* protons)

$\Delta E_{nn}(trans\rightarrow cis)$ is always given exactly if one knows the exact protonic arrangements. Thus the total perturbation energies of H_2O_2 and H_2 can be compared solely in terms of the electronic perturbation energies, $\Delta E_{el}^{H_2O_2}$ and $\Delta E_{el}^{H_2}$, which in turn may be analyzed through the transition densities, $\rho_{tc}^{H_2O_2}(1)$ and $\rho_{tc}^{H_2}(1)$ having the common Bonding and Antibonding Regions. *Fig.* 3 shows the contour maps of $\Delta v(1)$ depicted in Sections A, B, C, and D of the cylinder in *Fig.* 1. Because of the rather large absolute values of $\Delta v(1)$ in the vicinity of the protonic sites, the transition density near the sites would be expected to play the crucial role. The transition density contour maps in each section for H_2 and H_2O_2 are shown in *Figs.* 4 and 5, respectively. Since the y-axis of *Fig.* 1 is the

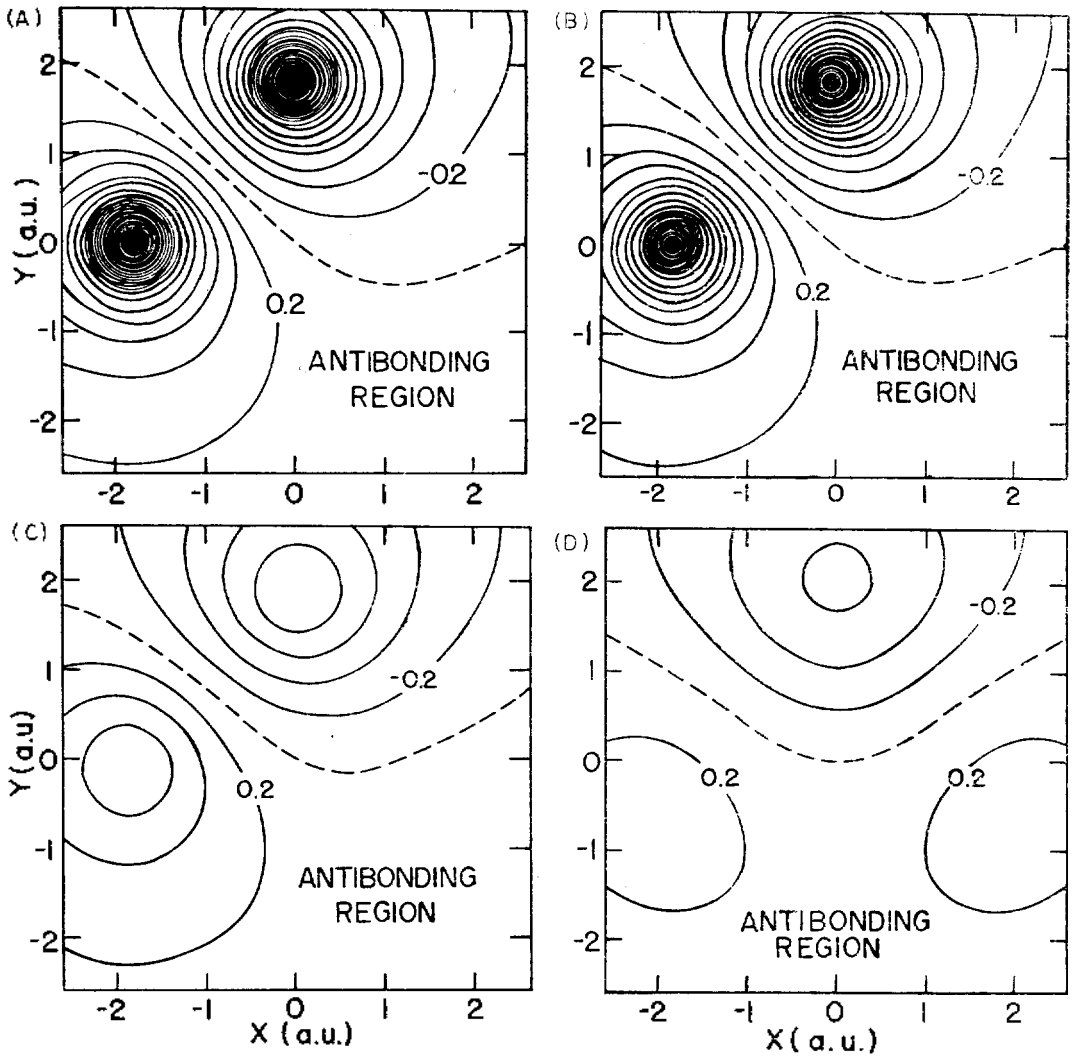

Fig. 3. Contours of $\Delta v(1)$ of H_2O_2 and H_2 in Sections A, B, C, and D. Contour intervals are -0.2 and 0.2 in the Bonding and Antibonding Regions, respectively. The dotted lines are the boundaries of two regions.

two-fold rotation axis, the maps in Sections G, F, and E are the mirror images of those in Sections A, B, and C, respectively. $\rho_{tr}^{H_2}(1)$ is normalized to 2 and $\rho_{tr}^{H_2O_2}(1)$ to 18, and thus the contour intervals are chosen with the different valuse: 0.01 a.u. for H_2 and 0.09 a.u. for H_2O_2. Therefore, the direct comparison of two maps is a little awkwared.

Fortunately, it can be easily shown, by the expansion of $\Delta v(1)$ in terms of the spherical harmonics, that an arbitrary density with cylindrical symmetry, $\rho_{cyl}(1)$, does not combine with the perturbation operator, $\Delta v(1)$, that is,

$$\int \Delta v(1)\rho_{cyl}(1)d\tau_1=0 \qquad (6)$$

The density, $\rho_{cyl}(1)$, may be the whole or a part of the cylindrical component of the transition density of H_2O_2, or the density of the oxygen molecule with the equivalent nuclear positions of oxygens in H_2O_2, or the superposed density of two atomic oxygens located

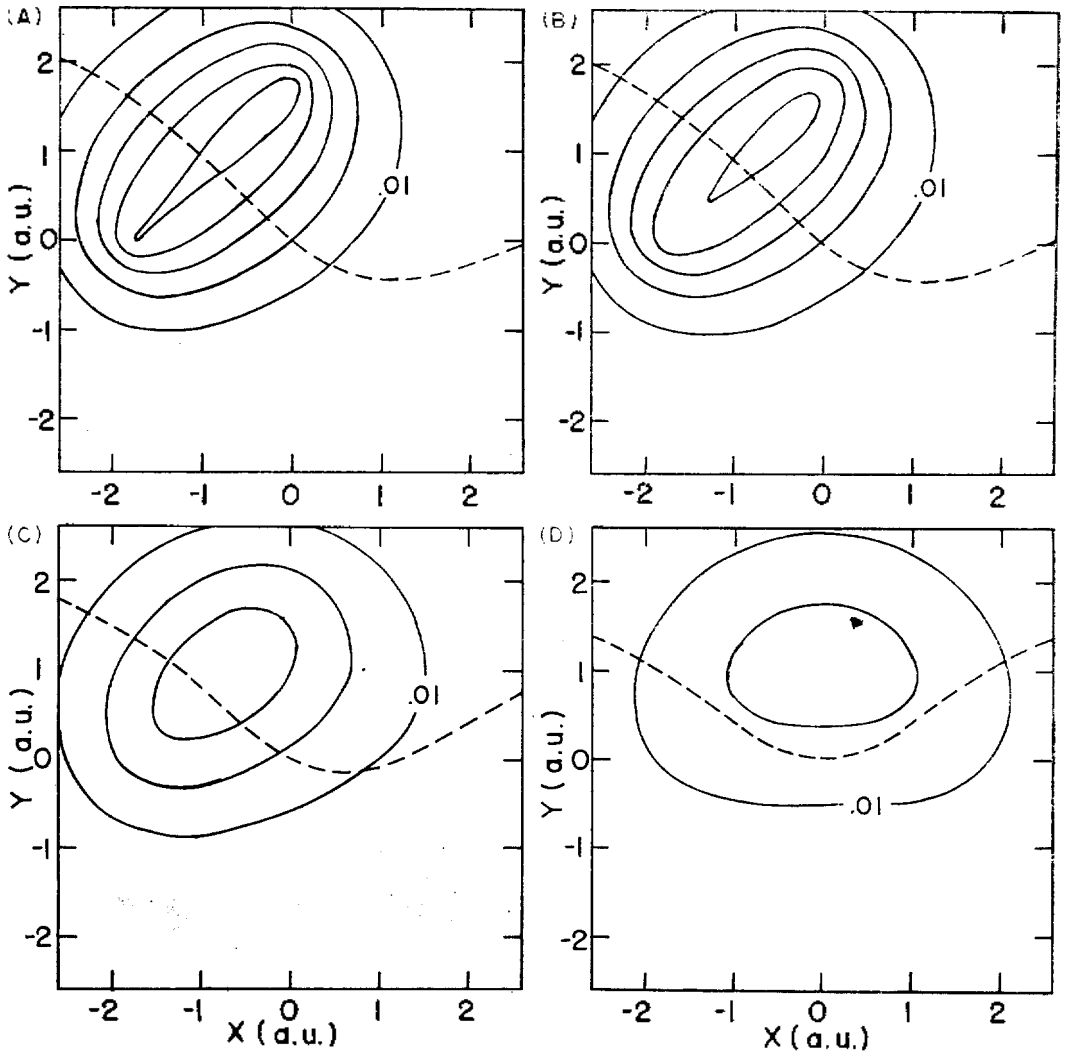

Fig. 4. Transition density of H_2, $\rho_{tr}^{H_2}(1)$, in Sections A, B, C, and D. Contour interval is 0.01 a.u. p-Orbitals in the wavefunctions by McLean *et al.* are not included.

at the same positions as in H_2O_2. If the effective transition density is defined as

$$\rho_{eff}^{H_2O_2}(1) \equiv \rho_{tr}^{H_2O_2}(1) - \rho_{cyl}(1) \tag{7}$$

one may write

$$\Delta E^{H_2O_2}(trans \rightarrow cis) = \int \Delta v(1) \rho_{eff}^{H_2O_2} d\tau_1 + \Delta E_{nn}(trans \rightarrow cis) \tag{8}$$

in place of Eq. (4). Substracting Eq. (3) from Eq. (8), the difference of the perturbation energies of H_2O_2 and H_2 accompanying the change from *trans* to *cis* is given by

$$\Delta E^{H_2O_2} - \Delta E^{H_2} = \int \Delta v(1) (\rho_{eff}^{H_2O_2}(1) - \rho_{tr}^{H_2}(1)) d\tau_1 \equiv \int \Delta v(1) \Delta\rho(1) d\tau_1 \tag{9}$$

where $\Delta\rho(1)$ is the difference between that effective transition density of H_2O_2 and the transition density of H_2, and will be called hereafter as the difference transition density. Because of the closeness of the normalizations of $\rho_{eff}^{H_2O_2}(1)$ and $\rho_{tr}^{H_2}(1)$, $\Delta\rho(1)$ may be visualized well on

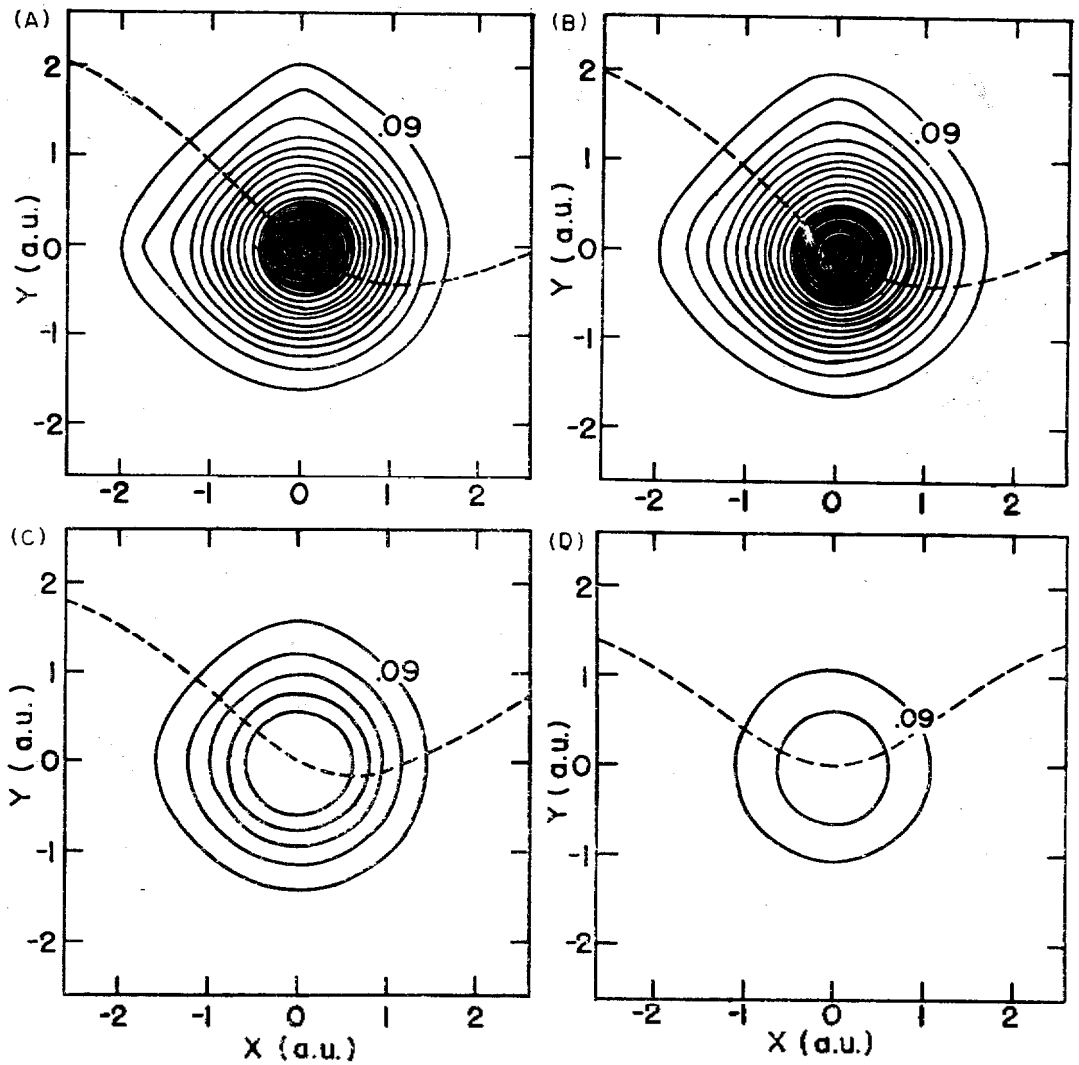

Fig. 5. Transition density of H_2O_2, $\rho_{tr}^{H_2O_2}(1)$, in Sections A, B, C, and D. Contour interval is 0.09 a.u.

plotting. In the present work, $\rho_{cyl}(1)$ is obtained from the square and cross terms of 1s, 2s, and $2p_z$, and from $2p_x^2+2p_y^2$ of oxygen atoms. It is normalized to circa 12. $\Delta\rho(1)$ is depicted in *Fig.* 6 and one observes the following from *Figs.* 4, 5 and 6:

(1) The transition density of H_2, $\rho_{tr}^{H_2}(1)$, is more heavily distributed in the Bonding Region than in the Antibonding Region. (See *Fig.* 4) The fact is thus clearly constistent with the large negative value of ΔE_{el}, −97.10 kcal/mole and with the observations in Paper I.

(2) Mostly positive contours of $\Delta\rho(1)$ in the central zones of each section (see *Fig.* 6) imply that $\rho_{tr}^{H_2O_2}(1)$ contracts toward the center of each section due to the strong O-H bonds. The strong O-H bond formations make the real charge density of H_2O_2 less dependent on conformations than that of H_2. Namely, the real charge densities of *trans* and *cis* H_2O_2 do not differ greatly from each other. The conjecture is also justified from the symmetrical shape (with respect to the boundary lines) of $\rho_{tr}^{H_2O_2}(1)$ in *Fig.* 5. In other words, $\rho_{tr}^{H_2O_2}(1)$, and therefore $\rho_{tr}^{H_2O_2}(1)$,

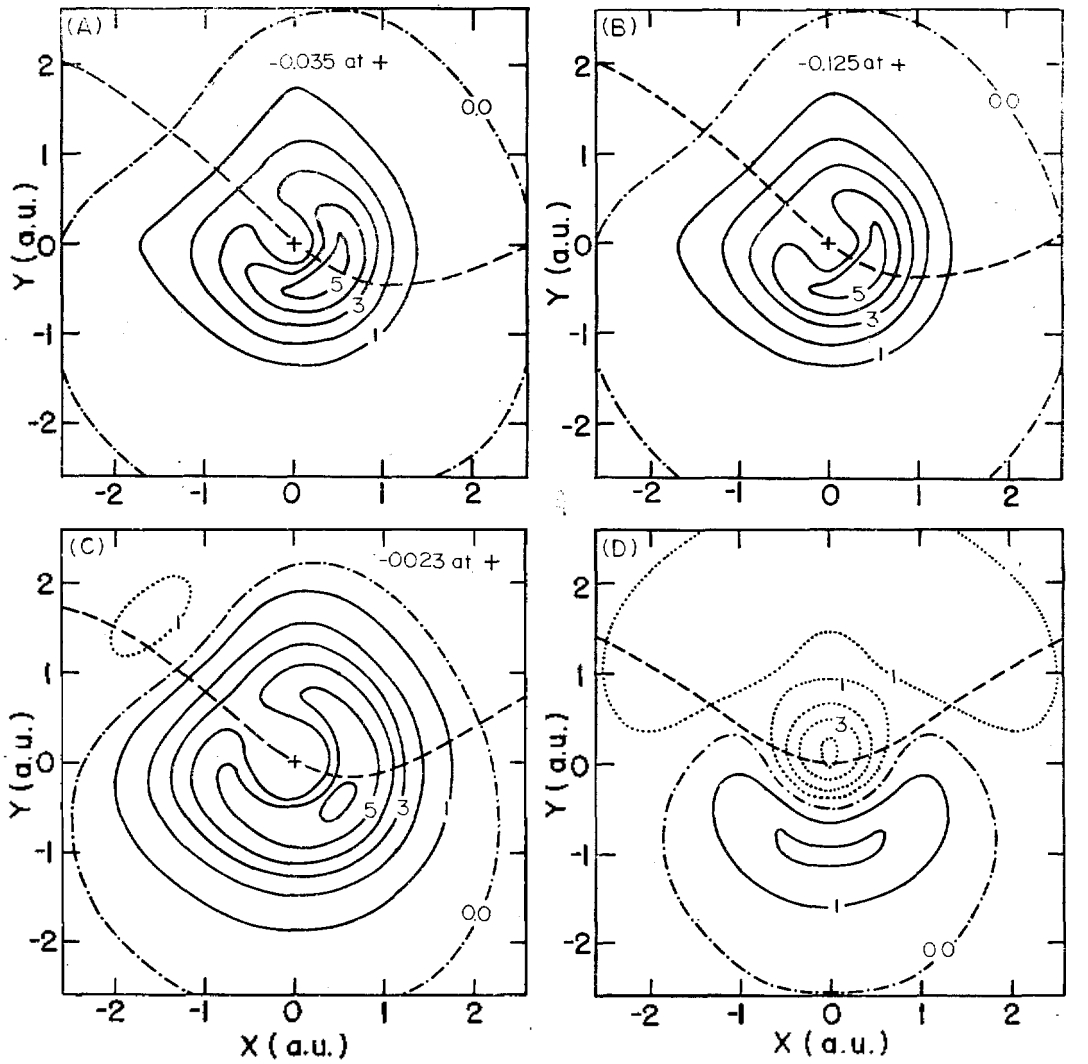

Fig. 6. Difference transition density, $\Delta\rho(1)$, in Sections A, B, C, and D. ——— is positive, – · – · – is zero, and ····· is negative contour. Contour 1: 0.1 a.u. in Sec. A and B, ±0.01 a.u. in Sec. C, and ±0.005 a.u. in Section D. Contour interval: 0.1 a.u. in Sections A and B, ±0.02 a.u. in Section C, and ±0.005 a.u. in Section D.

is less bonding than $\rho_{ic}^{tr}(1)$. Consequantly, the difference transition density in the Antibonding Region is distinctly dominant over that in the Bonding Region as one can see in *Fig.* 6. ΔE_{el}(*trans*→*cis*) is, however, still negative, since in the neighborhood of the protonic sites in the Bonding Region is slightly more excessive than that in the Antibonding Region, especially in sections A, B, and C.

From these observations, it may be concluded that a sharp rise of the electronic energy of H_2O_2 relative to H_2 during the change from *trans* to *cis* (39.71 kcal/mole, see *Table* 2), to such an extent that $|\Delta E_{el}| < |\Delta E_{nn}|$ in H_2O_2, can be understood in terms of the migration of the transition density from the Bonding Region to the Antibonding Region due to the strong bond formations between oxygen and hydrogen

on the same side.

It is, however, impossible to pinpoint the part of molecule which offers the major contribution to $\Delta E^{H_2O_2}-\Delta E^{H_2}$ since it depends on both $\Delta v(1)$ and $\Delta\rho(1)$. Futhermore, "the origin of the barrier to internal rotation" may be interpreted as the major and substantial cause of barrier formation at a certain dihedral angle, and in the case of H_2O_2, it is not ΔE_{el} but ΔE_{nn} which forms the barrier at the *cis* position. Introduction of an improved wavefunction may alter the numerical value of the barrier and may show both *cis* and *trans* barriers through the delicate balance of E_{el} and E_{nn}, but it would not change the qualitative picture of the transition density presented in this work.

In order to analyze the barrier of ethane, C_2H_6, from the similar viewpoint, the CNDO calculations on the hypothetical eclipsed and staggered H_6 molecules have been performed and the results are listed in *Table* 2. The electronic perturbation energy in ethane accompanying the change from staggered to eclipsed is smaller in magnitude than that in H_6, just as in the case of H_2O_2 *vs.* H_2. However, it fails to visualize the migration of the transition density to the Antibonding Region, because the very small difference of the perturbation energies of ethane and H_6, about 20 kcal/mole, and, in addition, the existence of six boundary surfaces make the contour lines of the transition bensity prohibitively delicate for visualization.

The transition densities both in the Bonding Region and in the Antibonding Region have the same symmetry properties as the perturbation operator, $\Delta v(1)$, and thus it would be rather inadequate to say simply that the origin of barrier is in a certain symmetry component of the transition density.[8]

4. CONCLUDING REMARKS

The origin of the barriers to internal rotation of hydrogen peroxide and ethane is analyzed in terms of the transition density. Adopting the hydrogen molecules which are strategically arranged in the space as reference, it is shown that the migration of the transition density to the Antibonding Region, due to the existence of the axial atoms, causes the decrease of the magnitude of the electronic perturbation energy to such an extent that the change of the nuclear-nuclear repulsion energy becomes the dominant portion of the total perturbation energy. The increase of the transition density in the Antibonding Region has its origin in the bond formations between the axial and end atoms on the same side. Thus the real charge densities of the molecules with axial atoms are less dependent on conformations than those of the hypothetical molecule having no axial atoms.

If each integral of Eq. (2) can be evaluated separately in any given part of molecule, for example, in each section with a finite thickness in *Fig.* 1, the concept of the Bonding and Antibonding Regions may be more useful even in the quantitative analysis of such problems involving the small electronic energy change as the rotation barrier of ethane.

ACKNOWLEDGEMENT

This research was supported by grant from the Ministry of Science and Technology under contract No. STF-77-39. The authors wish to think Professor Y. S. Kim and Professor C. W. Pyun for their helpful discussions. They are also much indebted to Professor K. Y. Choo for his making available the CNDO program. Computational services were provided by the Computing Center of the Seoul National University.

REFERENCES

1. J. D. Kemp and K. S. Pitzer, *J. Chem. Phys.*, **4**, 749 (1936).
2. R. M. Pitzer and W. N. Lipscomb, *J. Chem. Phys.*, **39**, 1995 (1963).
3. (a) U. Kaldor and I. Shavitt, *J. Chem. Phys.*, **44**, 1823 (1966); (b) L. Pedersen and K. Mokomura, *ibid*, **46**, 3941 (1967); (c) M. E. Schwartz, *ibid.*, **51**, 4182 (1969); (d) R. B. Davidson and L. C. Allen, *ibid.*, **55**, 519 (1971).
4. W. E. Palke and R. M. Pitzer, *J. Chem. Phys.*, **46**, 3948 (1967).
5. (a) W. H. Fink and L. C. Allen, *J. Chem. Phys.*, **46**, 2261 (1967); (b) *ibid.*, **46**, 2276 (1967); (c) *ibid.*, **47**, 895 (1967);
6. T. Nee, R. G. Parr, and R. J. Bartlett, *J. Chem Phys.*, **64**, 2216 (1976).
7. (a) W. L. Clinton, *J. Chem. Phys.*, **33**, 632 (1960); (b) M. Karplus and R. G. Parr, *ibid.*, **38**, 1547 (1963); (c) K. Ruedenberg, *ibid.*, **41**, 588 (1964).
8. R. E. Wyatt and R. G. Parr, *J. Chem. Phys.*, **41**, 3262 (1964); *ibid.*, **43**, S217 (1965); *ibid.*, **44**, 1529 (1966).
9. H. Kim and R. G. Parr, *J. Chem. Phys.*, **41**, 2892 (1964).
10. L. C. Allen, *Chem. Phys. Letters*, **2**, 597 (1968).
11. W. L. Jorgensen and L. C. Allen, *J. Amer. Chem. Sec.*, **93**, 567 (1971).
12. (a) O. J. Sovers, C. W. Kern, R. M. Pitzer, and M. Karplus, *J. Chem. Phys.*, **49**, 2592 (1968); (b) C. W. Kern, R. M. Pitzer, and O. J. Sovers, *ibid.*, **60**, 3583 (1974).
13. (a) R. M. Stevens and M. Karplus, *J. Amer. Chem. Soc.*, **94**, 5140 (1970); (b) G. F. Musso and V. Magnasco, *J. Chem. Phys.*, **60**, 3754 (1974); (c) E. Lombardi, G. Tarantini, L. Pirola, L. Jansen and T. Ritter, *ibid.*, **61**, 894(1974); (d) M. Levy, T. Nee and R. G. Parr, *ibid.*, **63**, 316 (1975); (e) P. A. Christiansen and W. E. Palke, *ibid.*, **67**, 57 (1977).
14. H. Kim and D. Lee, *J. Korean Chem. Soc.* **23**, 15 (1979). Paper I of the present series.
15. P. O. Lōwdin, *Phys. Rev.*, **97**, 1474, 1490 (1955).
16. $\Delta v(1)$ and ΔV_{nn} are the perturbation operators of nuclear-electron attraction and nuclear-nuclear repulsion, respectively.
17. A. D. McLean, A. Weiss, and M. Yoshimine, *Rev. Mod. Phys.*, **32**, 211 (1960).
18. R. H. Hunt and R. A. Leacock, *J. Chem. Phys.* **45**, 3141 (1966). Experimental *cis* and *trans* barriers are 7.08 and 1.10 kcal/mole, respectively. Equilibrium dihedral angle is about 111°.
19. E. A. Mason and M. M. Kreevoy, *J. Amer. Chem. Soc.*, **77**, 5808 (1955).
20. R. L. Redington, W. B. Olson and P. C. Cross, *J. Chem. Phys.*, **36**, 1311 (1962).